WCTE 2020
WORLD CONFERENCE ON TIMBER ENGINEERING
SANTIAGO, CHILE | 24 - 27 AUGUST

# A NEW INTEGRATED APPROACH ON THE SEISMIC STRENGTHENING OF EXISTING RC BUILDINGS WITH EXTERNAL CROSS-LAMINATED TIMBER PANELS

**Lorenzo Badini[1], Stephan Ott[1], Patrik Aondio[1], Stefan Winter[1]**

**ABSTRACT:** In this study a timber-based integrated solution is presented to solve at once common issues affecting typical reinforced concrete (RC) existing buildings, such as seismic and energy performances, providing an eco-friendly alternative to steel external bracing systems. Cross-laminated timber (CLT) walls are provided perpendicularly to the external façades as strengthening elements while interposed CLT slabs are foreseen at each floor level to host new architectural units together with a new envelope. While the connections to the foundations and to the existing RC frames are provided respectively with traditional brackets and simple axial-connectors distributed along the height of the building, a post-tensioned connection, between CLT panels (PT-CLT connection), is implemented in the system to guarantee resistance to horizontal actions acting parallel to existing façades with consequent structural independence and architectural freedom. A numerical model is developed with finite element software and non-linear static analyses with target displacement checks are performed to assess the seismic improvement obtained. Finally, the preassembled architectural components that allow to renovate the envelope and the provided assembly procedure are revealed.

**KEYWORDS:** Cross-laminated timber, existing building, seismic retrofit, target displacement, energy retrofit

## 1 INTRODUCTION

The renovation of existing building stock is an increasingly important topic, due to the progressive deterioration of the major part of the buildings, designed and realized between the 50's and the 90's. The European Union counts about 200 million existing units, representing around 27% of total energy consumption [1]. Furthermore, many of these are located in seismically active areas and designed without any reference to horizontal loads or follow outdated standards. This is the main context of Pro-GET-onE research and innovation project, whose main objective is the design, verification and assessment of an integrated technological system to be assembled externally to existing reinforced concrete (RC) structures in order to obtain a seismic and energy improvement that at the same time offers additional space for extended housing units [1]. The structural seismic improvement has been proven with a steel three-dimensional exoskeleton [2, 3]. Seismic analyses have been performed through FEM software before and after the application, to existing RC structures, of the strengthening steel-based exoskeleton, showing that the increase in strength and stiffness of the entire building is usually associated with an increase in capacity and a reduction of ductility. Complementary to the external structure, architectural components are developed for the extensions of the building envelope [1, 4, 5]. The pre-assembled solutions had to face the challenges of architecture variability (extra-room, sunspace, and balcony), completing the strengthening structure, and were provided as prefabricated boxes or slabs composed by combinations of cross laminated timber (CLT) panels and wooden frames. Together with the increased space delivered by the extension of the exoskeleton, airtightness, insulation, and new façade is provided by the components. These interventions result in higher energy efficiency, renewal of the building envelope, thus updated asset value [1]. Combined with new and efficient heat, ventilation, and air conditioning (HVAC) systems, their piping, and the inclusion of renewable energy sources (RES) on the roof, the architectural components aim to achieve the level of nearly zero energy building [6-8]. Worth mentioning are also the contributions that address the environmental impact of the project [9, 10], comparing different scenarios within the prototype-renovation and against the process of demolition and rebuild. From the LCA it is calculated that over a period of analysis of 50 years, out of a total of about 700 tonnes of $CO_{2e}$ related to the whole renovation, 35% is due to the external steel structure. It is clear that to further address climate change mitigation and minimise the environmental impact, alternative structural solutions should be investigated.

In the last decades, as consequence of an accelerated drive towards sustainable materials, the rediscovery of wood as a structural material has led to the spread of new engineering wood products and related research (citing only mass timber products, laminated veneer and

[1] Lorenzo Badini, lorenzo.badini@tum.de
[1] Stephan Ott, ott@tum.de
[1] Patrik Aondio, aondio@tum.de
[1] Stefan Winter, winter@tum.de
all: Technical University of Munich, Chair of Timber Structures and Building Construction, Germany

strand lumber and cross-laminated timber). In particular, CLT panels are produced to a high degree of prefabrication which allows efficient and safe on-site installation and they have been applied globally in many low-rise and mid-rise buildings typically using platform construction technology [11]. Under seismic loads, CLT shear walls with properly designed connection systems are able to provide adequate lateral capacity for multi-storey buildings. Despite the lightness of the material which allows to have low values of mass, a higher level of lateral in-plane strength and stiffness can be reached [12]. These qualities make it a product that is easily applicable for extensions [13, 14] or renovation of existing buildings [15-21].

In Slovenia, Sustersic I. and Dujic B. evaluated a new system for combined seismic retrofit and energy efficiency that exploited the CLT panels applied in parallel to the façades of an existing RC-building [15]. The CLT jacket, depending on the dimensions of the applied panels, reveals itself as a not invasive intervention that is rigidly connected to the RC frames by means of angular brackets nailed to the wood and fixed with bolts to the concrete slabs. It proved to increase stiffness and strength of the entire existing RC structure without influencing the global ductility. Furthermore, the CLT panels can be upgraded with various insulation types implying an integrated energetic renovation. The same system was then developed and optimised on RC frames and in combination with masonry unreinforced structures, where through the variation of the bonding system or the connectors, an increase in ductility was provided. Furthermore, the system has demonstrated the possibility of increasing the performance of already severely damaged structures [16-18]. In this context, from the University of Venice (IUAV), studies were conducted in order to characterise layering configurations applied on CLT-strengthening panels, taking into account minimisation of heat-losses, environmental impacts and intervention costs [19]. More recently, a similar solution has been proposed in [21] that foresees again an outer shell made of CLT panels combined with an insulation layer within additional timber framework. Simulations on the system have demonstrated the reduction on energy demand, technical details are aimed at developing a pre-assembled system that can be easily assembled from the outside with dry components, exploiting a new friction-based dissipative connection between the panels and the RC frames. Finally, confined and unconfined CLT panels were studied also as new infills for RC frames showing a substantial reduction in lateral displacement complemented by higher peak load capacity [20].

The study presented in this article will describe an innovative and integrated system that together with energetic and structural improvements, entails the possibility of increasing the volume of existing buildings with consequent increased value of the real estate that could further mitigate the renovation costs.

## 2 INTEGRATED SYSTEM

In accordance with the philosophy of the EU project, it was necessary to develop an integrated system capable of satisfying all the three principal objectives (seismic safety, energetic improvement, and additional space). By means of external performing façades or extensions, prefabricated wooden components can easily be installed with effective results [22, 23].

Within the contents of Pro-GET-onE three case studies are provided: a moment-resisting RC frame located in Athens (Greece), a hybrid masonry-RC structure in Bagnolo in Piano (Italy), a precast concrete walls structure in Brasov (Romania). The latter has been chosen as reference structure due to the climatic conditions of the area, and the local availability of wood. It is a five-stories social housing block of flats, characterised by a superstructure made of prefabricated RC walls (Figure 1). More information about this case study is reported in [24, 25]. In the report, needs for energy and architectural improvement were highlighted, in contrast with a general good performance concerning the seismic vulnerability assessment. For this reason, the integrated timber-based system was developed as architectural independent extension for the case study, providing a complete energy renovation of the envelope. A virtual moment-resisting RC structure designed for vertical loads only and with a morphology as close as possible to the Romanian case study (considering some spanning changes due to a different structural system) was then numerically investigated in combination with the timber-based strengthening system to prove the seismic improvement. All the data related to the RC frames are reported in chapter 3 as description of the initial state FEM model (Figure 13).

***Figure 1:*** *Photo of the precast-concrete walls case study in Brasov*

CLT walls constitute the structural strengthening system for the existing structure and are externally added in continuity of the RC frames, in the plane perpendicular to the external façades. They improve the seismic performance increasing the global stiffness of the system, reducing the displacement demand, and increasing the capacity by avoiding concentration of damages in the lower levels. CLT slabs are then provided horizontally creating a “bookshelf” in which

the different architectural solutions are provided, guaranteeing the new performing envelopes (Figure 2).
While the vertical walls are made of 200 mm thick CLT panels composed of five layers of birch (40-40-40-40-40) [26], the slabs are made of 160 mm CLT spruce panels with five layers (40-20-40-20-40) and are connected at each floor by means of a moment-resisting post-tensioned connection that adapts the analytical behaviour presented by F. Wanninger and A. Frangi [27, 28]. The strength values of the timber CLT are summarised in Table 1.

***Table 1:*** *Characteristic strength and stiffness properties in MPa for CLT-Spruce (ETA-06/0009 – EN 338) and CLT-Birch [26], plus relative mean density values in kg/m³*

| Value | Units | CLT-Spruce | CLT-Birch |
|---|---|---|---|
| $f_{m,CLT,k}$ | MPa | 24 | 38 |
| $f_{c,0,CLT,k}$ | MPa | 21 | 38 |
| $f_{c,90,CLT,k}$ | MPa | 2.5 | 5.0 |
| $f_{t,0,CLT,k}$ | MPa | 14 | 28.5 |
| $E_{0,CLT,mean}$ | MPa | 12,000 | 15,000 |
| $E_{90,CLT,mean}$ | MPa | 370 | 650 |
| $G_{CLT,mean}$ | MPa | 690 | 710 |
| $\rho_{CLT,mean}$ | kg/m³ | 470 | 620 |

Both the connections to the foundations and to the existing structures are made with consolidated and simplified solutions in order to minimise the uncertainties on the numerical analyses and leaving space for further research development.
Every wall has been connected to the foundation level with 12 angular brackets (BMF116) and 16 hold-downs (HTT22), distributed on both side of the 2 m width CLT panels.
The connection with the existing structure is designed to transmit only the axial loads acting in direction perpendicular to the existing façade, allowing the interaction between the two structures only for horizontal actions acting in-plane to the CLT walls.

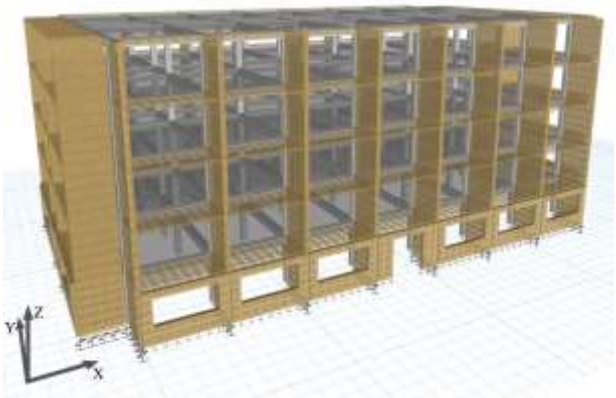

***Figure 2:*** *Finite element model of the CLT-based strengthening system applied to four sides of the building*

## 2.1 PT-CLT-CONNECTIONS

Adapting concepts and principles originally developed for precast concrete construction [29], post-tensioned (PT) timber systems have been developed and tested since 2005 at the University of Canterbury [30]. The technology takes advantage of unbonded post-tensioned steel tendons passing through internal cavities in timber beams or walls to create a moment resisting connection. The seismic demand is satisfied through controlled rocking between structural elements and tendon elongation, which also ensures recentering capabilities. Thus, energy-dissipation devices (replaceable mild steel components, viscous or friction dampers) could be provided creating hybrid connections characterised by the typical flag-shaped behavioural law (see Figure 3). For the sake of brevity a complete state of the art on Pre-Lam technology is not summarised here, but reference is made to [31].

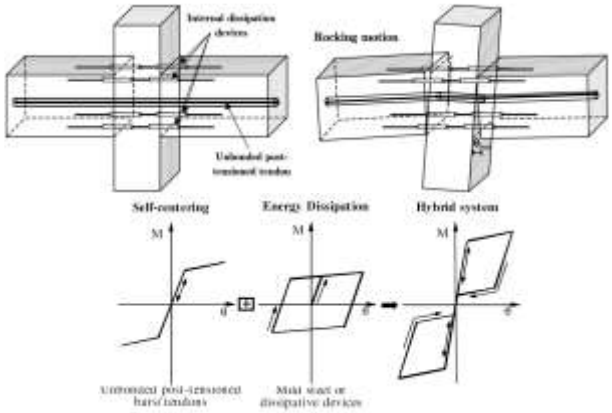


***Figure 3:*** *Above the application of hybrid concept to LVL frame systems [30]; below the idealised flag-shape hysteresis loop [30]*

As mentioned in the previous section, direct reference to the analytical method reported in [27, 28] was made for the adaptation of the PT connection to CLT panels.
With difference from the New Zealand experience, at the ETH Zurich the PT frames are developed with glulam made from Norway spruce, and present a reinforcement made of European ash where high stresses perpendicular to grain occur (column and bottom side of the beams), avoiding the use of steel reinforcements in the joints. Extensive experimental testing have been performed under both gravity and lateral loads, on single column-beam subassemblies, an entire three-spans frame and ending with the construction of a prototype [32].

***Figure 4:*** *On the left glulam column-beam specimen; above on the right the entire three-spans frame and below the first floor of the ETH House of Natural Resources [32]*

The analytical model is based on springs that represent the softer column and only bear compressive forces. The beam ends at the interface and behave like a rigid body

due to the higher strength and stiffness of the timber components in parallel to grain direction. Hence, the model corresponds to a (stiff) foundation on (soft) ground (Winkler theory) [27]. Since there are no dissipating elements, a gap occurs in the interface as soon as there is no compression at either the top or bottom edge of the connection. The analytical model describes the behaviour of the connection (moment-rotation), and based on equilibrium of forces and bending moments at the interface, leads to three stages that depend on the value of the neutral axis $x$ (Figure 8 and 9) [27, 33]:

1. Before decompression ($x=h$); the beam is in full contact with the column. Linear behaviour.
2. After decompression ($x<h$); a gap occurs at the edge of the beam. Non-linear behaviour.
3. Tendon elongation ($x<h/2$); when the neutral axis goes below the tendon, the latter gets elongated, resulting in an increase in tendon force and stiffness. Non-linear behaviour with increased slope.

Asymmetrical loads imply shear deformations in the column that depend on the eccentricity of the resultant compressive forces on the two interfaces of the joints. This occurs in the outer joints and more significantly in the inner ones when subject to horizontal loads as shown in Figure 5.

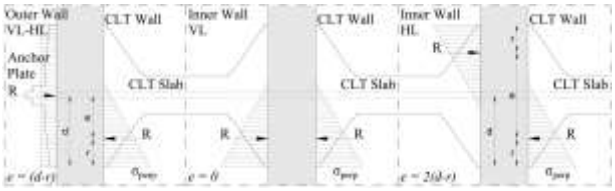


***Figure 5:*** *Distribution of stresses at the connection interfaces of outer and inner walls in the cases of vertical and horizontal loads (VL, HL)*

The transition from a beam-column system with linear elements to a system with two-dimensional elements involved the use of a composite steel plate to increase the contact surface between horizontal and vertical elements maintaining adequate rotational stiffness (depending on the hight of the horizontal element) without encountering a premature failure of the grain compressed perpendicularly (Figure 6).

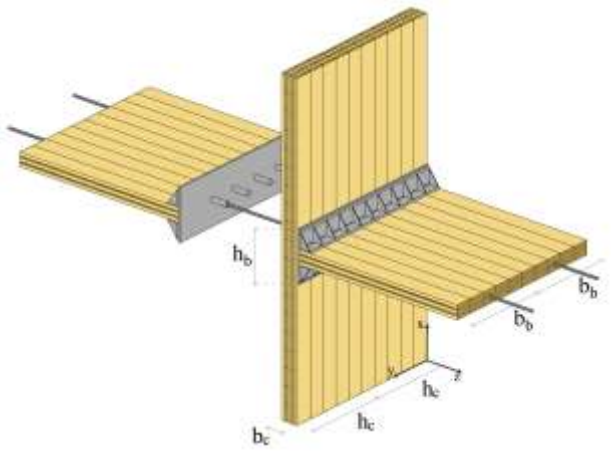


***Figure 6:*** *PT-connection between CLT panels by means of steel unbonded cables and steel composed plates*

This connection steel plate is composed by a large steel plate 20 mm thick, with two angular brackets L 200 mm x 150 mm x 18 mm and four steel pipes (Figures 6 and 7). The large plate with the L-profiles allows to increase the height of the horizontal element for the evaluation of the rotational behaviour while the steel pipes are inserted in specific holes of the CLT vertical element to transfer the vertical loads. The holes in the CLT provide tolerances allowing a relative rotation of the plate, and the steel pipes must overlap one another during the assembly of inner joints ($\phi$48.3 mm x 2.6 mm and $\phi$60 mm x 2.16 mm). Reinforcing LVL made of hardwood is provided at the contact interface between the horizontal CLT element and the smaller side of the angular steel profile to avoid the crushing of the grain. Alternatively, a stiffer external layer could be already provided manufacturing the CLT slabs. The steel unbonded tendon passes through the horizontal elements along their development and across the vertical one. It is composed by four wired strands with cross sectional area about 600 mm$^2$, Young's modulus of 197 GPa and a maximal tension strength about 1,770 MPa (ETA-13/0810 in [34]).

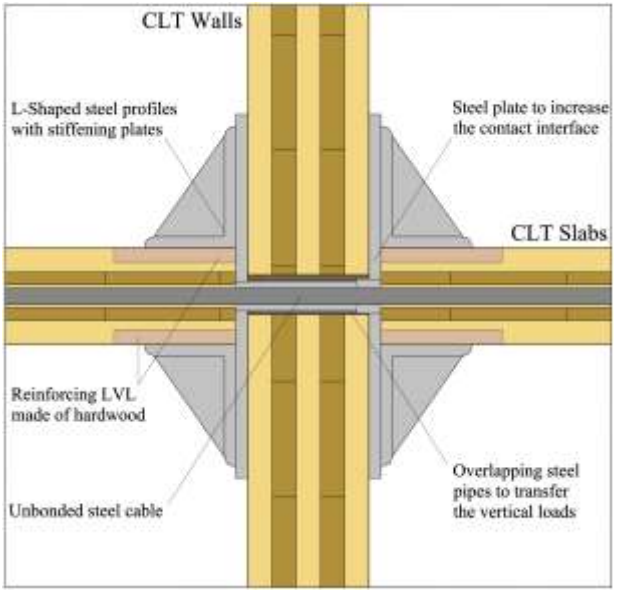


***Figure 7:*** *Detail of the PT-CLT connection with steel plates*

Through this system the analytical model presented in [27, 28] was adapted. In table 2 a comparison between the input data used for the calculation of the rotational spring is reported with reference to the notations of Figure 6. $S_{xz}$ represent the shear rigidity of the CLT in the *xz* plan as calculated in [35].

***Table 2:*** *Comparison between the values used in [27], referring to a column specimen made of ash, and the CLT vertical element made of birch. These inputs were used for the calculation of the rotational behaviour (half of the total depth)*

| Value | Units | D40 [27] | CLT-Birch |
|---|---|---|---|
| $E_{90,mean}$ | MPa | 860 | 650 |
| $G_{0,mean}$ | MPa | 810 | - |
| $S_{xz}/b_c$ | MPa | - | 246 |
| $f_{c,90,k}$ | MPa | 8.3 | 5 |
| $b_c$ | mm | 280 | 200 |
| $h_c$ | mm | 600 | 1,000 |
| $b_b$ | mm | 400 | 1,000 |
| $h_b$ | mm | 600 | 600 |

Through the adaptation of the analytical model, it was possible to obtain the laws describing moment, compression perpendicular to grain in the vertical element, neutral axis position and tension in the tendon in relation to the rotation at the interface. Below in Figures 8 and 9 the first two relationships mentioned above are shown with reference to half of the depth of the system (1 m with one steel cable) and an initial tension ($P_0$) set to 500 kN. It is evident, especially from Figure 8, how much relevant is the shear deformation of the CLT vertical element on the rotational stiffness.
Finally, it is important to mention that the analytical model developed in [27] was particularly precise until the phase of tendon elongation. In this phase the analytical model was losing precision, overestimating the stiffness [27]. However, for the purpose of this study, the connection is meant to stay in the elastic range under the design seismic loads. Thus, allowing the exploitation of the analytical model without experimental coefficients.

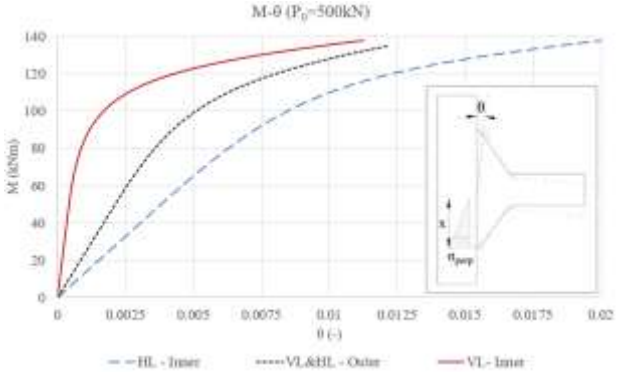


***Figure 8:*** *Moment-rotation behaviour of the PT-CLT connection calculated for the inner elements with vertical loads (VL) and horizontal loads (HL) and for the outer elements*

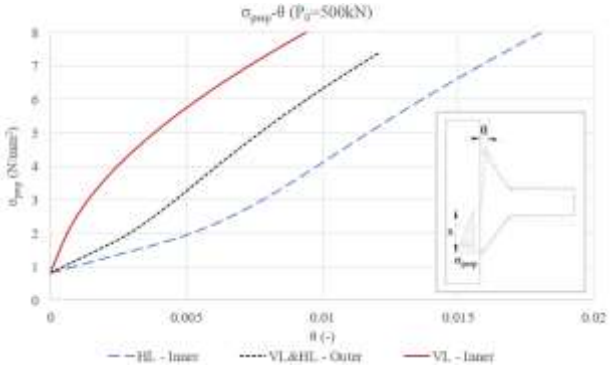


***Figure 9:*** *Compression perpendicular to grain in relation to the rotation at the PT-CLT connection interface, calculated for the inner elements with vertical loads (VL) and horizontal loads (HL) and for the outer elements*

A specific series of tests will be performed soon in order to prove the adaptation of the analytical model to CLT element by means of steel plates.

## 2.2 CONNECTORS AT FOUNDATION LEVEL

The use of hold-downs and angular brackets as connectors for CLT structures is widely spread in construction practice and extensively investigated in research [12, 36-38]. Due to this reason typical connectors were exploited at the foundation level distributed on both sides of the CLT walls. With specific reference to [36] commercial products already characterised by linear strength properties, secant stiffness and non-linear behavioural laws were provided:

- 12 angular brackets (BMF 90 mm x 48 mm x 3 mm x 116 mm) fastened to the CLT walls with 12 nails (or screws) $\phi$ 4 mm / 60 mm and with 2 M12 bolts to the foundation were provided in the middle of the walls as shear anchors with a contribution also to prevent up-lift loads (see Figure 10);
- 16 hold-downs (HTT22) fastened to the CLT each with 22 nails (or screws) $\phi$ 4 mm / 60 mm and with 1 M12 bolt to the foundation were placed towards the corners of the walls to resist overturning forces (Figure 10).

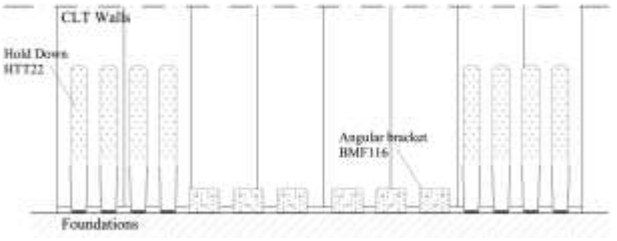


***Figure 10****: Multiple connectors at foundation level are represented in the drawing on one side of the CLT wall*

The friction at the foundation level was calculated considering the vertical loads coming from the quasi-permanent load combination. Due to the lightweight of the material and the limited dimensions of the external CLT structure, the axial loads in the walls are limited with a consequent small relevance of the friction at the base. Considering a friction coefficient between wood

and concrete of 0.62, the contribution of friction is calculated and exposed below in Table 3.

***Table 3:*** *Activated friction forces at the bottom of the inner and outer walls*

| Value | Units | Inner wall | Outer wall |
|---|---|---|---|
| $N$ | kN | 110.3 | 68.09 |
| $F_{fr}$ | kN | 68.4 | 42.2 |

Despite the rapid implementation of the connectors in the numerical model (see Figures 16, 17, 18), the right number of connectors was determined iteratively, checking the force-displacement relationship during non-linear static analysis, matching the seismic global safety of the intervention while keeping the connectors (especially the hold-downs located at the edge of the walls) within their maximum allowed displacement.

### 2.3 CONNECTION WITH THE EXISTING STRUCTURE

As mentioned before the connection with the existing structure is designed to transmit only axial loads acting in-plane to the CLT walls. Twenty connectors are distributed along the height of the building, consisting of steel rods ($\phi$ 12 mm / 150 mm) fixed with chemical dowels to the CLT walls and providing steel plates to be anchored at the vertical RC elements (see Figure 11). The threaded galvanised rod made of reinforcing steel (B450C) is characterised by a bilinear stress-strain relationship as shown in Figure 15.

This steel connector plate must provide specific tolerances that allows relative vertical and horizontal displacements. While the relative vertical displacement results in maximum of 5 mm (a tolerance of 10 mm is provided), the horizontal displacement is more significant; considering the roof displacement of the short side (more flexible) under seismic loads, and asynchronous vibration modes, it can reach 100 mm. The fixation of the steel plate to the RC elements is hypothesised from the façade plane with bolts chemically anchored to the RC. Particular attention on this connection must be paid for a realistic application. It is in fact important to have a reliable level of knowledge of the structural existing elements and materials in order to rely on chemical fixations. Additionally, a careful evaluation of the extra loads applied on the columns must be done. Depending on the existing elements, the steel plate may be connected to a steel reinforcing jacketing of the external RC columns to avoid local collapses. In order to transfer compressive loads between the RC frames and the CLT walls and so avoiding instability in the bars, hardwood components will be provided in-between the steel connectors.

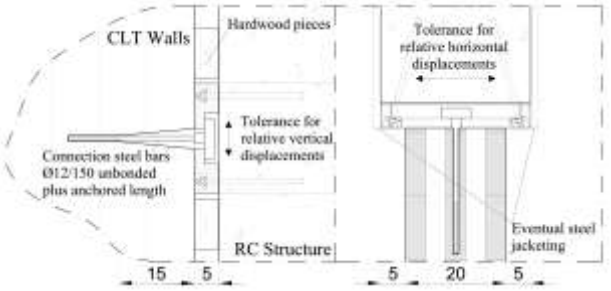


***Figure 11:*** *Sketches of the vertical distributed connection between CLT walls and RC vertical structural elements*

During the installation procedure the steel bars could be already fixed to the CLT walls and arrive at the construction site with the steel plates in position for the fixation to the RC elements.

## 3 FINITE ELEMENT MODEL

A numerical model was developed with the finite element software ETABS [39] both for the existing RC structure alone (initial state – IS) and for the combined solution with the CLT external structure. Through linear dynamic (modal response spectrum) and non-linear static (pushover) analyses, it was subsequently possible to assess the seismic improvement.

### 3.1 INITIAL STATE – EXISTING STRUCTURE

The existing moment-resisting RC structure is developed based on the existing case study of Brasov and located in the same area. The structure consists of five floors of 2.6 m height each with a total plan size of 28 m x 15 m measured from the barycentric axes of the frames. The horizontal structures are made of 120 mm thick concrete slabs that can be considered as diaphragm constraints transferring the vertical loads in both the main directions. The beams have different heights depending on the spans, and a width that corresponds to the side of the columns. These vertical elements are 350 mm x 350 mm at the ground floor and 300 mm x 300 mm for the remaining storeys. The spans between columns are following the morphology of the reference Brasov structure, but adapting the dimensions to the different structural system. Along the longitudinal direction (X) the frame presents 7 spans of 4 m, while in the transversal direction (Y) two spans of 6 m are interrupted by a single 3 m span (see Figure 12). The dimensions of the structural elements and the amount of reinforcement are designed based exclusively on vertical loads, with stresses coming from the ultimate limit state combination as defined by the Eurocodes [40, 41]. The cross-sectional dimension of the structural elements together with the reinforcement content are indicated in Table 4. In addition to dead loads, including weights coming from the various masonry infill and partition walls, live loads referred to residential building were considered.

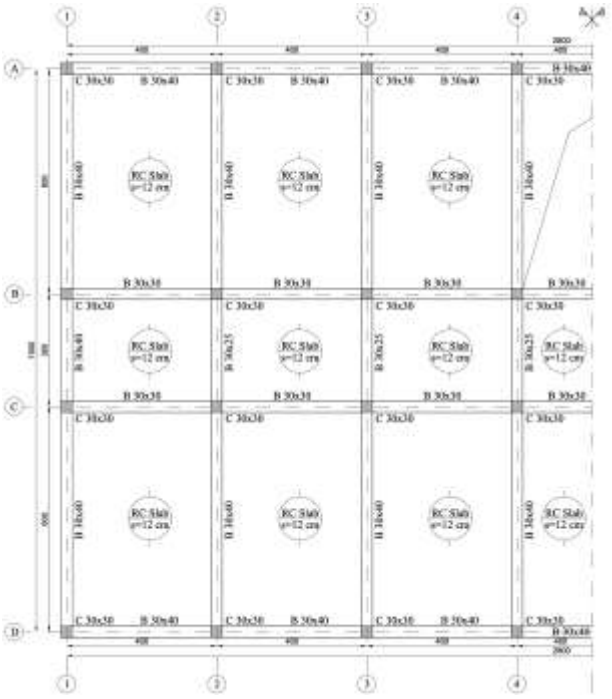

***Figure 12:*** *Typical horizontal cross section of the moment-resisting structure. Due to the symmetry of the structure only half of the planimetry is shown. Cross-sectional dimensions of beams (B) and columns (C) are indicated together with spans*

***Table 4:*** *Cross-sectional dimensions of beams (B) and columns (C) are indicated in the table together with the relative reinforcement content and spanning lengths*

| Cross-section | Span | Long. Rebar | | Trans. Rebar |
|---|---|---|---|---|
| mm | m | Top | Bottom | ϕ/step (mm) |
| C 350x350 | 2.6 | 3ϕ18 | 3ϕ18 | ϕ8/200 |
| C 300x300 | 2.6 | 2ϕ18 | 2ϕ18 | ϕ8/200 |
| B 350x400 | 4 | 3ϕ14 | 3ϕ14 | ϕ8/200 |
| B 350x400 | 6 | 2ϕ18<br>1ϕ14 | 3ϕ14 | ϕ8/200 |
| B 350x250 | 3 | 3ϕ14 | 3ϕ14 | ϕ8/200 |
| B 350x300 | 4 | 3ϕ14 | 3ϕ14 | ϕ8/200 |
| B 300x400 | 4 | 3ϕ14 | 3ϕ14 | ϕ8/200 |
| B 300x400 | 6 | 2ϕ18<br>1ϕ14 | 3ϕ14 | ϕ8/200 |
| B 300x250 | 3 | 2ϕ14 | 2ϕ14 | ϕ8/200 |
| B 300x300 | 4 | 3ϕ14 | 2ϕ14 | ϕ8/200 |

As regards of the FEM concrete class C20/25 ($f_{ck,cyl}$ = 20 MPa) and steel grade PC52 ($f_{yk} \geq$ 355 MPa) were used with reference to the technical assessment report provided by the municipality of Brasov in the framework of Pro-GET-onE [25].

A three-dimensional model was created to carry out the seismic analyses (Figure 13). Fixed joints were introduced at the foundation level as external restrains and diaphragm semi-rigid constraints were introduced for all the joints belonging to the floor levels. Beams and columns were modelled as nonlinear frame elements with lumped plasticity by defining plastic hinges at both ends of the elements. The hinge properties follow the formulas reported in the Annex A of the Eurocode 8-Part 3 [42] for ductile mechanisms and can identify the performance levels for each step of the non-linear static analysis (see paragraph 4). The behaviour of these hinges is depending on the cross-section of the element, the material properties, the longitudinal and transversal steel reinforcements, and the axial loads level calculated with a quasi-static combination of vertical loads. ETABS provides default-hinge properties and PMM (combined flexural and axial loads) hinges for columns and M3 (only flexural loads) hinges for beams were assigned. In order to take into account brittle failures on the same elements, force-controlled hinges were placed in the middle of each column and at the ends of each beam (V2 for beams and V2-V3 for columns). The shear strength, which is the maximum allowable force for these hinges, is calculated with reference to the paragraph 6.2.3 of [40].

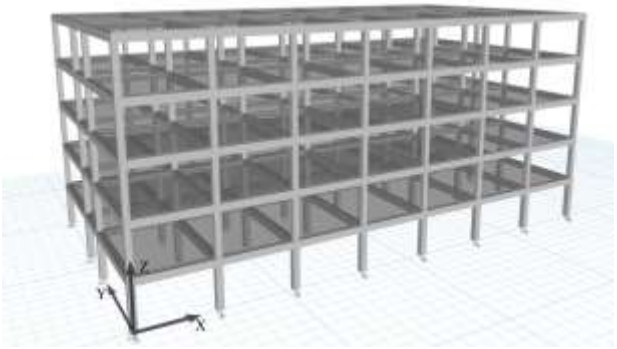

***Figure 13:*** *Finite element model of the initial state (RC moment-resisting structure)*

As unique difference between the non-linear model and linear one a consideration was made on the concrete cracking. On this purpose, in the linear model a property modifier is reducing beam and column shear and flexural stiffnesses of 50% as indicated in [43].

### 3.2 PROJECT STATE – CLT STRUCTURE

As mentioned above the CLT walls are placed in the same plane of the RC frames and are increasing the performance against horizontal loads acting in-plane to the walls. In the longitudinal direction, the two systems remain independent. Therefore, to obtain an improvement in both the main directions, the CLT external structure must be provided on the entire perimeter as shown in Figure 2.

In the numerical model the CLT panels are realised with shell layered elements that provides crossed layers of the implemented timber orthotropic material (CLT made of birch and spruce as defined in Table 1). The correct behaviour of the CLT panels is checked based on [35, 44]. Basic FEM models were created to verify the possibility of using shell layered elements as CLT panels. The deformations due to out-of-plane loads, the torsional stiffness, the stability with second order effects and the in-plane shear stiffness were carefully compared with hand-calculations. All these numerical tests gave good results with variations in displacements below the 2% apart for the deformations due to out-of-plane loads. In fact, the shell layered elements follow a Kirchhoff formulation and as stated in [44] do not consider the shear rigidity $S_{xz}$ with an error that is decreasing with the length of the element (higher slenderness). Therefore, to

take into account the shear deformation, a reduction of the modulus of elasticity is applied at the orthotropic material imputed for the various layers depending on the static scheme of each considered element.
Multi-linear springs with linear stiffness and relative linear and non-linear behavioural laws are implemented in the model to represent the various connectors involved (PT-CLT-connections, hold-downs, angular brackets, steel fixating rods) and the activated friction.
The PT-CLT-connection was implemented in the FEM with rotational springs (see Figure 14, on the right) characterised by the behavioural law (moment-rotation) illustrated in Figure 8 and a linear stiffness calculated considering angular coefficient of the line in the elastic phase (see Table 5). Since shear deformations were relevant only for horizontal loads, two models were developed independently with PT-CLT connections set respectively for vertical loads (ultimate limit state, ULS and serviceability limit state, SLS) and horizontal loads (significant damage limit state, LS-SD and damage limitation limit state, LS-DL). The 2 m depth shell-layered elements, representing the CLT structural elements, were regularly divided in four parts creating five joints at the edges. The stiffness of each spring (five for each PT-CLT-connection) is determined considering double of the depth of the single 1 m system (multiplying by 2) and then assigning $1/5^{th}$ to each spring located at the connecting side. In the same way the moment-rotation behaviour is distributed along the rotational springs.

***Table 5:*** *Rotational effective elastic stiffness of the PT-CLT connections referred to 1m CLT structure*

| Value | Units | Inner PT-connection | Outer PT-connection |
|---|---|---|---|
| $k_{vert.loads}$ | kNm/rad | 117,000 | 23,565 |
| $k_{horiz.loads}$ | kNm/rad | 13,102 | 23,565 |


***Figure 14:*** *On the left FEM-scheme of the steel fixating rod connection between RC columns and CLT walls; on the right FEM-scheme of the PT-CLT inner connection*

The connection with the existing structure is realised in FEM with a multi-linear spring with a linear stiffness as reported in Table 6 and an axial linear and non-linear behaviour as represented in Figure 15. Twenty connectors are provided along the height of the entire structure (four per storey) and connected to the joints of the CLT-shell elements and to rigid links representing the thickness of the RC columns (left scheme in Figure 14).

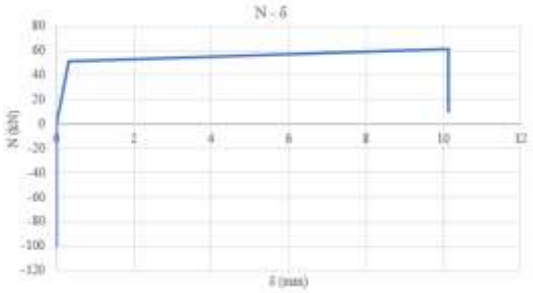


***Figure 15:*** *Envelope and load bearing capacity of the steel rods applied as axial connectors. While the tensile behaviour is characterised by the tensile capacity of the ϕ12/150 rod, the compressive transfer is guaranteed by the hardwood pieces*

Regarding the foundation connectors, a series of rigid links is provided at the final side of the shell layered element to adjust the shell subdivisions with the multi-linear springs representing angular brackets, hold-downs, and friction (see Figure 16). While angular brackets (BMF116) are characterised by behavioural laws describing deformations under axial and shear loads, the hold-downs (HTT22) only present the first component. To simplify the model, the springs representing the hold-downs also contain the friction contribution (divided by the number of springs considered along the length). The envelope and load bearing capacity of these connectors are shown in Figures 17 and 18 for single connector with reference to [36].

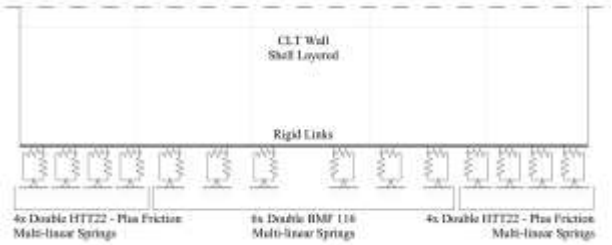


***Figure 16:*** *FEM-scheme of the connectors provided at the base of the shell layered CLT wall on one side*

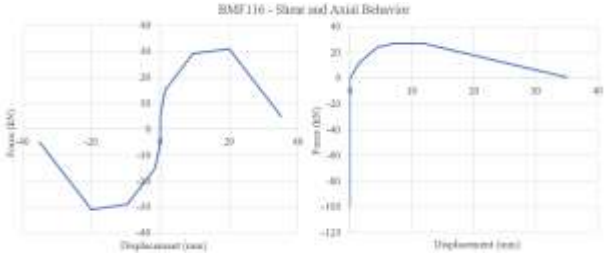

***Figure 17:*** *Envelope and load bearing capacity of the shear anchor with 12 nails of ϕ 4 mm / 60 mm when acting in shear (left graph) and with axial loads (right graph)[36]*

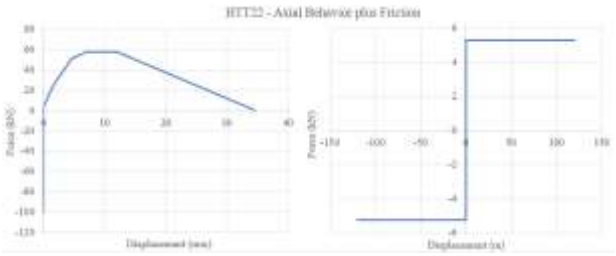

***Figure 18:*** *Envelope and load bearing capacity of the hold-down with 22 nails of ϕ 4 mm / 60 mm for preventing up-lifting (left graph) and 1/8 of the friction contribution*

In the FEM, forces and linear stiffnesses of the connectors have been doubled because of a double number of connectors intended to be applied on both sides of the CLT walls.

***Table 6:*** *Values of the elastic stiffness of the steel connecting rods (ϕ12), single and double angular brackets (BMF116)[36] and hold downs (HTT22)[36]; friction is neglected in linear analyses*

| Value | Units | Tensile strain | Shear strain |
|---|---|---|---|
| $k_{\phi 12}$ | kN/m | 158336 | - |
| $k_{BMF116}$ | kN/m | 5000 (10000) | 8000 (16000) |
| $k_{HTT22}$ | kN/m | 11250 (22500) | - |

It is important to mention that in linear analyses the axial behaviour of the connectors cannot be represented correctly due actual non-linear behaviour from tension to compression. Therefore, since the deformation in the model is twice the one of a real in-plane loaded CLT wall (considered as rigid body, see Figure 18), the axial linear stiffness of the connectors has been doubled.

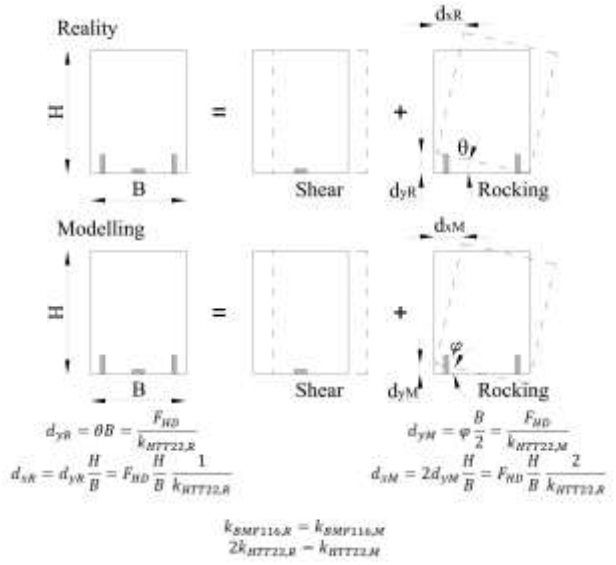


***Figure 19:*** *Connector's stiffnesses, determination of the axial linear equivalent stiffness to use in the FEM*

## 4 SEISMIC ANALYSES

Modal response spectrum dynamic linear analyses (RSAs) and static non-linear pushover analyses (SPOs) were carried out before and after the application of the timber-based addition on the basis of the provisions of the Eurocode 8 [43]. While RSAs were used to design the new structural elements and connections, reporting the stresses affecting them in the different design load combinations (ULS, SLS and LS-SD), SPOs allowed to assess the level of seismic vulnerability before and after the structural strengthening, thus determining the obtained improvement.

A type 1 elastic response spectrum on ground type A was matched (see Figure 20) with the use of the database provided in [45], characterised by a peak ground acceleration of 0.2 g with a return period of 475 years ($P_r$ = 10% in 50 years), and then modified with a soil factor B as indicated in the available technical report [25]. Based on the elastic response spectrum different design spectra were defined depending on the different q-factors, obtained with the SPOs (differentiated by directions and state of the project) and reported in Table 8. The stresses belonging to the RSAs were combined with a quasi-permanent combination of vertical loads and verified for each CLT panel (slabs and walls) as indicated in [35, 46]. Furthermore, also ULS and SLS combinations were checked using, as mentioned in previous paragraphs, two different models based on different rotation springs representing the PT-CLT connections.

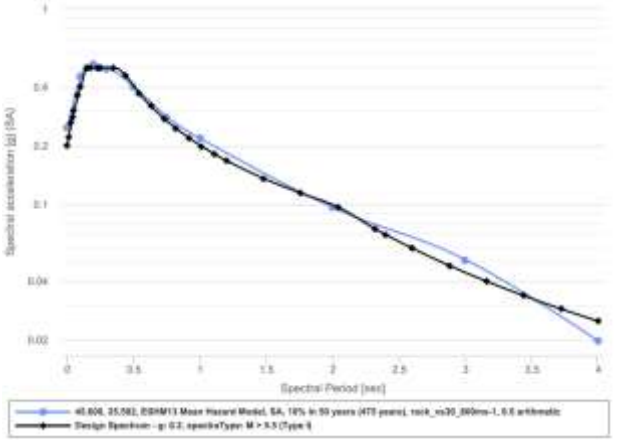

***Figure 20:*** *Registered elastic response spectrum of Brasov (45.600-25.582) with matching EU8 spectrum [43, 45], [www.efehr.org/Documentation/licenses-copyright](www.efehr.org/Documentation/licenses-copyright)*

In the same way, all the forces affecting the connectors were checked (hold-downs, angular brackets, PT-CLT connections and steel bars), resulting in the satisfaction of the requirements. The only exception was related to some external hold-downs that would have required an increased number of nails with a consequent increased stiffness and an additional iteration of the design not included in this study. In Table 7 the maximum forces affecting the connectors are shown together with the strength capacity (both with 22 and 26 nails for the axial capacity of the hold-downs).

***Table 7:*** *Maximum forces obtained with the RSA at the LS-SD for the different components of the connectors: steel connecting rods (ϕ12), angular brackets (BMF116) and hold downs (HTT22); the capacities are also reported considering a $k_{mod}$ of 1.1 and a $\gamma_m$ of 1.3*

| Value | Units | Max. Force | Capacities |
|---|---|---|---|
| $N_{\phi 12}$ | kN | 55.00 | 61.07 |

| | | | |
|---|---|---|---|
| $V_{BMF116}$ | kN | 9.32 | 23.44 |
| $N_{BMF116}$ | kN | 7.98 | 21.62 |
| $N_{HTT22\_22n}$ | kN | 47.11 | 46.54 |
| $N_{HTT22\_26n}$ | kN | - | 55.00 |

With the displacements obtained through the RSA analyses was possible to check the interstorey drift ($d_r$) before and after the application of the timber strengthening solution for both the main directions following 4.4.3.2 of [43]. As shown in Figure 21, the interstorey drifts of the centres of masses (CM) resulted beyond the design requirements for the initial state and verified in the project solution.

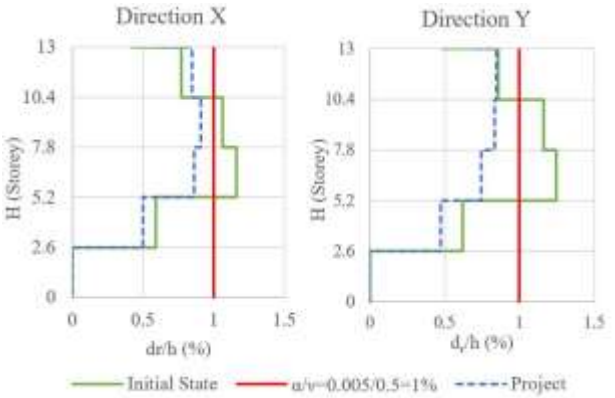


***Figure 21:*** *Storey drifts control for both directions before and after the project application*

A force controlled static non-linear analysis based on the quasi-permanent vertical loads combination constitutes the starting point for the displacement-control pushover analyses (SPOs). The latter were performed, as required by the standards [43], in both direction, with positive and negative signs and using two different lateral load distributions: proportional to mass regardless of elevation and proportional to the lateral forces associated to the main vibrating modes. As results, capacity curves associating the total base shear acting at each loading step with the displacement of the control point, situated in the roof, are derived for the multi degree of freedom (MDOF) model. Below, in Figure 22, the capacity curves of the structure before and after the application of the timber addition are shown for both the main directions and with a distribution of forces proportional to modal shapes.


***Figure 22:*** *Capacity curves obtained with the SPO proportional to the lateral forces associated with the vibrating modes for both the main direction with before and after the project*

Finally, by using the target displacement verification (TDV) as defined in the Annex B of [43], the displacement capacity is evaluated for which the performance level of significant damage limit state was exceeded for the elements of the existing RC structure. The target displacement is found with the scaled capacity curves representing the equivalent single degree of freedom (SDOF) system and the elastic response spectrum of the site for the LS-SD. Figure 23 represents the TDV for the pushover acting in transversal direction (Y) with a distribution of forces proportional to masses.

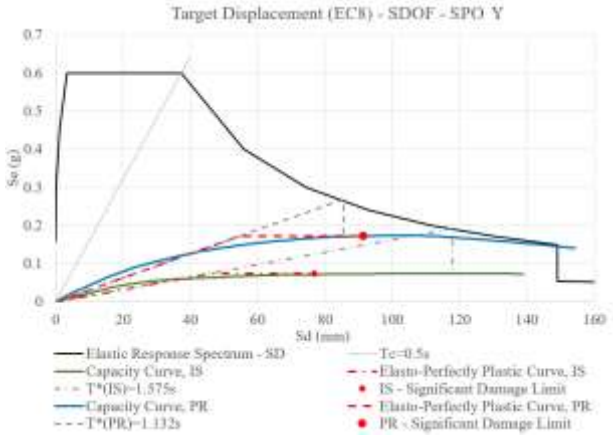


***Figure 23:*** *Pseudo-acceleration and displacement elastic response spectrum (0.2 g), SDOF capacity curves with relative elasto-perfectly plastic curves and indicating displacement capacities, period values; through T* and the elastic response spectrum the demanded displacements are also defined*

Considering the elastic response spectrum introduced above, it was possible to evaluate the ratio between capacity and demand for all the assessed combination, obtaining an improvement that goes, in the weakest lateral load distribution (modal force distribution), from 62% to 101% in transversal direction (Y), and from 66% to 102% in the longitudinal one (X).

***Table 8:*** *Target displacement verification for the significant damage performance level (LS-SD), $T_R$ = 475 years, $P_V$ = 10% in 50 years. Capacities and demands are expressed in mm of the control points for the analyses that regard the initial state (SPO) and the project (P-SPO)*

| Analyses | Capacity | Demand | C/D (%) | q |
|---|---|---|---|---|
| SPO X | 90.1 | 126.6 | 71 | 2.62 |
| SPO -X | 88.4 | 124.6 | 71 | 2.59 |
| SPO MX | 96.7 | 147.1 | 66 | 2.66 |
| SPO M-X | 99.4 | 146.5 | 68 | 2.64 |
| SPO Y | 89.2 | 136.9 | 65 | 2.55 |
| SPO -Y | 85.7 | 133.5 | 64 | 2.55 |
| SPO MY | 99.4 | 160.7 | 62 | 2.60 |
| SPO M-Y | 98.7 | 159.3 | 62 | 2.60 |
| P-SPO X | 129.3 | 114.3 | 113 | 1.68 |
| P-SPO -X | 127.3 | 113.1 | 113 | 1.69 |
| P-SPO MX | 143.8 | 139.1 | 103 | 1.79 |
| P-SPO M-X | 142.5 | 139.7 | 102 | 1.80 |
| P-SPO Y | 119.9 | 110.4 | 109 | 1.54 |

| | | | | |
|---|---|---|---|---|
| P-SPO -Y | 118.1 | 109.0 | 108 | 1.53 |
| P-SPO MY | 135.2 | 131.3 | 103 | 1.62 |
| P-SPO M-Y | 131.7 | 130.3 | 101 | 1.60 |

As shown in Table 8, all the seismic analyses resulted satisfied in the project solution mostly due to an improved distribution of damages inside the existing structure as shown in Figure 24. In fact, in the project solution a uniform shear deformation occurs over the entire height of the building; while previously, the first floor was primarily loaded.

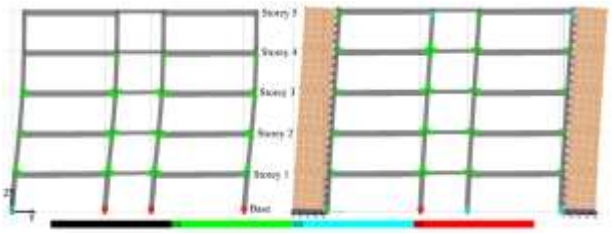

***Figure 24:*** *Deformed shapes of the SPOs in transversal direction before and after the project application; the coloured dots represent the status of the plastic hinges*

Finally, to measure the exploitation of the external structure the amounts of horizontal force taken by both the RC and the CLT structures were derived for the SPOs at the step of the LT-SD (Table 9) highlighting a margin of improvement of the system that could be explored in further steps by varying the base connection system.

***Table 9:*** *Total horizontal forces at the step identifying the LS-SD and respective RC and CLT components with exploitation percentages of the external strengthening solution*

| Analyses | Total (kN) | RC (kN) | CLT (kN) | % |
|---|---|---|---|---|
| P-SPO X | 4,145 | 2,597 | 1,548 | 37 |
| P-SPO MX | 3,108 | 2,573 | 535 | 17 |
| P-SPO Y | 5,284 | 3,292 | 1,991 | 38 |
| P-SPO MY | 4,204 | 3,253 | 951 | 23 |

## 5 TECHNOLOGICAL SOLUTIONS

The technological solutions were designed based on the objectives of Pro-GET-onE, optimising the pre-fabrication of the components and the assembly procedure, guaranteeing efficient energy performance with a user-oriented approach.
Thanks to the use of prefabricated wooden elements and post-tensioned connections the assembly procedure of the structure is designed to be fast and practical. The steel connection plates constitute a useful temporary support for the slabs until application of the tension and the lightness of timber means reduction of time and costs. In order:

- CLT walls are fixed to the foundations (suitably designed based on the morphology of the existing ones, design loads and soil condition);
- steel plates without the upper angle profile and providing steel pipes as shear keys are inserted in specific holes in the CLT walls;
- horizontal CLT slabs are lifted on top of the steel L-shaped profiles;
- cables are inserted and the steel composite plate closed with the upper L-profile;
- the entire system is tensioned and the CLT panels at the ground floor are installed.

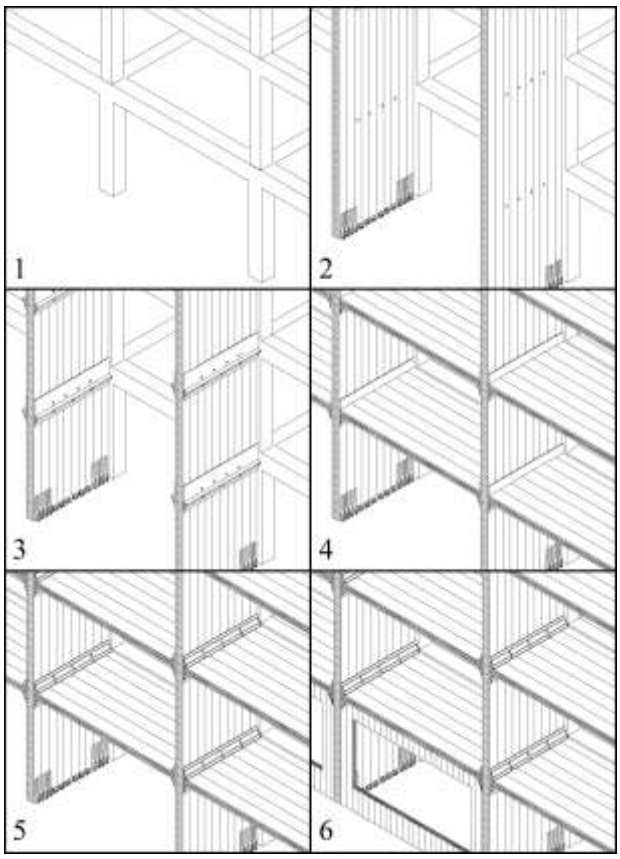


***Figure 25:*** *Sketches representing the steps of the assembly procedure of the structure*

It is important to underline the disruption that could be generated during the construction of the foundations and the application of the connectors to the existing RC columns that could be related to a local strengthening.
Subsequently three architectural solutions are provided in direct collaboration with the CLT panels, extra-room (Figure 26), sunspace, and balcony. For each solution, the design guarantees thermal conductivity performances (U-value) suitable for a nearly zero energy building (Table 10). Pre-assembled façade components are therefore provided: an external wooden frame insulated panel for the extra-room and a technical beam integrated with railings, stringcourse and gutter for balcony and sunspace. In the last two cases, the new envelope is provided on the existing surface and can be easily installed exploiting the external structure.

***Table 10:*** *conductivity values associated to the external vertical partitions, designed to stay below the limit value of 0.24 W/m²K*

| Walls | Positioning | U (W/m²K) |
|---|---|---|
| Prefabricated timber-based walls | Extra-room | 0.196 |
| Insulated RC | Balcony and | 0.232 |

| | | |
|---|---|---|
| frames | Sunspace | |
| Insulated masonry infills | Balcony and Sunspace | 0.155 |

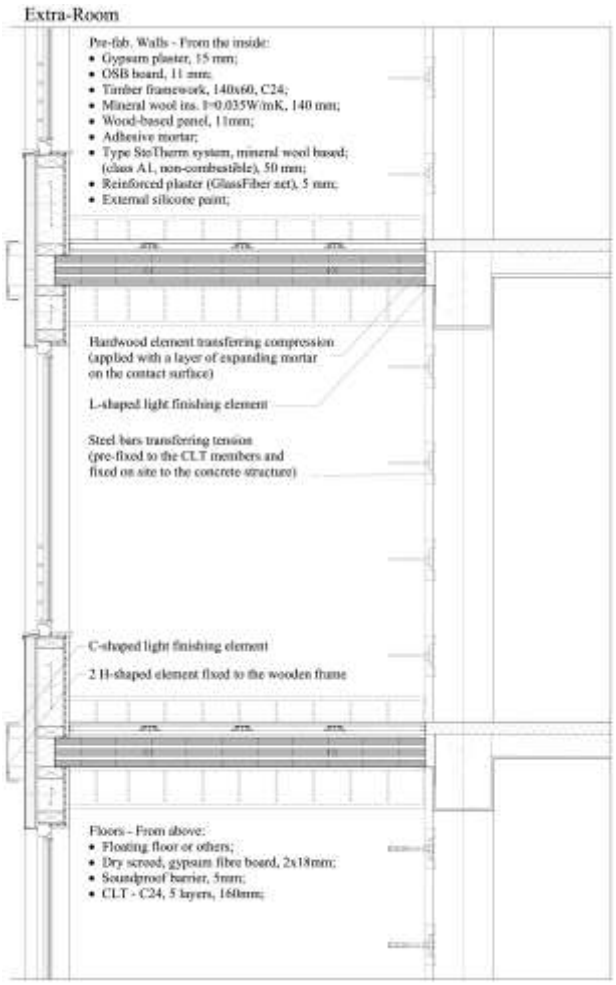


***Figure 26:*** *Detail of the extra-room architectural solution provided within the external CLT strengthening structure; the prefabricated timber-based walls, providing window frames are easily inserted in between the CLT slabs and fixed to the main structure from the front*

Two main issues were encountered in the adopted architectural solutions. The first regards the light reduction inside the existing units, that could be solved exploiting particular devices distributing the light from the frontal openings, such as light shelfs [47]. The second depends on the case study and its usable height. Characteristic of this particular case study, and of many similar residential building stocks, is the limited interstorey height, often defined in order to comply with the minimum usable height required by regulations by virtue of an optimised design. Consequently, where the height of the structural existing slabs (RC) is lower than the floor of the new addition (CLT), there will be a decrease in this height. To minimise this problem, it is therefore necessary to at least standardise the architectural solutions adopted for each façade, avoiding the installation of insulation at every additional floor, and closing off the heated cores either outside the addition (all extra-rooms) or on the edge of the existing façades (variable balcony or greenhouse).

# 6 CONCLUSIONS

The contribution aims to introduce and describe a new integrated technology made out of timber engineering products (CLT panels) to ensure an energy and architectural retrofitting connected at the same time to a structural improvement. It has been proven to be able to answer the three main requirements of the European project Pro-GET-onE, providing an efficient and more sustainable alternative to the more established steel exoskeletons.

To exploit the geometry of the addition maintaining architectural freedom and speeding up the assembly procedure a PT connection between CLT panels is provided through an adaptation of the analytical method proposed in [27]. Further mechanical tests on this topic are ongoing at the Technical University of Munich.

FEM of the structures were provided for the initial state and for the project solution to verify the new structural elements and to assess the seismic improvement obtained on a RC moment-resisting structure located in Brasov (Romania). The results of the analyses show that this timber-based external structure could be comparable to a steel exoskeleton [3] satisfying the design displacement values associated to the performance level of significant damage. Furthermore, verifications for the limit state of damage limitation, in terms of interstorey drifts got satisfied after the application of the integrated system.

However, the horizontal forces derived from the capacity curves at performance level of significant damage indicated that globally the CLT walls take from 17% to 38% from the total amount, showing margins of improvement for further steps. In order to increase the global stiffness and consequently improving the performance against frequent earthquakes, the insertion of steel prestressed cables within the layers of the CLT walls (vertically) could be investigated [48, 49]. An increased stiffness at the foundation interface between the CLT walls and the concrete could then be provided exploiting the rocking mechanisms, with a consequent reduction of connectors. Additionally, the insertion of dissipative devices at the level of the connections with the existing structure could decrease the global seismic demand. The current selection of connectors was, in fact, intended to minimise the variables in the numerical analyses.

Finally, a rapid assembly procedure concerning the structure is shown to underline advantages of using lightweight timber products, with respect to steel or concrete counterparts, and the level of prefabrication of the various elements with a consequent optimization of construction time. With the same logic prefabricated technological architectural solutions constitute the finishing “layer” of the renovation, providing an efficient energetic envelope and three possibilities of spacing units.


# ACKNOWLEDGEMENT

This article is part of the Pro-GET-onE project which has received funding from the European Union’s

Horizon 2020 Innovation action under grant agreement No 723747.

## REFERENCES


1. Ferrante, A., G. Mochi, G. Predari, L. Badini, A. Fotopoulou, R. Gulli and G. Semprini. "A european project for safer and energy efficient buildings: Pro-get-one (proactive synergy of integrated efficient technologies on buildings' envelopes)." *Sustainability* 10 (2018): 812. https://www.mdpi.com/2071-1050/10/3/812.
2. Fotopoulou, A., L. Badini, G. Mochi, G. Predari, R. Roijakkers and R. Cojocaru. "Seismic strengthening through external exoskeleton." *TEMA* 4 (2018): 18. https://doi.org/10.17410/tema.v4i3.203.
3. Badini, L., C. A. De Stefano, A. Custodi, G. Predari and A. Ferrante. "Seismic strengthening of existing rc structure through external 3d exoskeleton." Presented at IABSE Congress, New York City, 2019, New York, 2019. 114, 1018-24. 10.1080/10168664.2019.1599209.
4. Ott, S. and M. Krechel. "Construction principles of seismic and energy renovation systems for existing buildings." *TEMA* 4 (2018): 15. https://doi.org/10.17410/tema.v4i3.205.
5. Fotopoulou, A., A. Ferrante, L. Badini, G. Predari, G. Mochi, G. Semprini, R. Gulli, M. Assimakopoulos and D. Papadaki. "An integrated system for façade additions combining safe, energy efficient and userorientated solutions " *TEMA* 5 (2019): 10. https://doi.org/10.17410/tema.v5i1.216.
6. Assimakopoulos, M.-N., R. F. De Masi, D. Papadaki, S. Ruggiero and G. P. Vanoli. "Energy audit and performance optimization of a residential university building in heating dominated climates of italian backcountry " *TEMA* 4 (2018): 15. https://doi.org/10.17410/tema.v4i3.202.
7. Ferrante, A., A. Fotopoulou, G. Semprini, D. Cantelli, S. Ruggiero, M. Karalis, C. Efthymiou, D. Papadaki and M.-N. Assimakopoulos. "Ieq and energy improvement of existing buildings by prefabricated facade additions: The case of a student house in athens." Presented at 2019. 609, 042047. 10.1088/1757-899x/609/4/042047.
8. Barmparesos, N., D. Papadaki, M. Karalis, K. Fameliari and M. N. Assimakopoulos. "In situ measurements of energy consumption and indoor environmental quality of a pre-retrofitted student dormitory in athens." *Energies* 12 (2019): 2210. https://www.mdpi.com/1996-1073/12/11/2210.
9. Guardigli, L., M. A. Bragadin, A. Ferrante and R. Gulli. "Life cycle analysis and planning in the renovation process of public housing " *TEMA* 5 (2019): 14. https://doi.org/10.17410/tema.v5i2.232.
10. Guardigli, L., C. Ferrer, C. Peters, A. Fotopoulou, M. A. Bragadin and A. Ferrante. "Rehabilitation of public housing buildings in a life cycle perspective." Presented at 2019. 296, 012038. 10.1088/1755-1315/296/1/012038.
11. Dangel, U. "“tall wood buildings: Design, construction, and performance” by michael green and jim taggart." *Technology|Architecture + Design* 2 (2018): 254-56. 10.1080/24751448.2018.1497379. https://doi.org/10.1080/24751448.2018.1497379.
12. Dujic, B., T. Assistant and R. Zarnić. "Shear capacity of cross-laminated wooden walls." (2008):
13. Sustersic, I., B. Dujic and S. Gostič. *Timber upgrade of structures on seismically active areas*. 2010,
14. Hristovski, V., B. Dujic, N. Naumovski and M. Garevski. *Shaking-table tests and comparative numerical investigation of various upgrade systems on existing rc structures*. 2018,
15. Sustersic, I. and B. Dujic. "Seismic strengthening of existing buildings with cross laminated timber panels." World Conference on Timber Engineering 2012, WCTE 2012, 2012. 4,
16. Sustersic, I. and B. Dujic. *Seismic strengthening of existing urm and rc structures using xlam timber panels*. 2013,
17. Sustersic, I. and B. Dujic. "Seismic strengthening of existing concrete and masonry buildings with crosslam timber panels." Presented at Dordrecht, 2014. Materials and Joints in Timber Structures. S. Aicher, H. W. Reinhardt and H. Garrecht. Springer Netherlands, 713-23.
18. Sustersic, I. and B. Dujic. *Seismic shaking table testing of a reinforced concrete frame with masonry infill strengthened with cross laminated timber panels*. 2014,
19. Mora, T. D., A. Righi, F. Peron and P. Romagnoni. "Functional, energy and seismic retrofitting in existing building: An innovative system based on xlam technology." *Energy Procedia* 82 (2015): 486-92. https://doi.org/10.1016/j.egypro.2015.11.851. http://www.sciencedirect.com/science/article/pii/S1876610215026119.
20. Stazi, F., M. Serpilli, G. Maracchini and A. Pavone. "An experimental and numerical study on clt panels used as infill shear walls for rc buildings retrofit." *Construction and Building Materials* 211 (2019): 605-16. https://doi.org/10.1016/j.conbuildmat.2019.03.196. https://www.sciencedirect.com/science/article/pii/S0950061819306853.
21. Margani, G., G. Evola, C. Tardo and E. M. Marino. "Energy, seismic, and architectural renovation of rc framed buildings with prefabricated timber panels." *Sustainability* 12 (2020): 4845. https://www.mdpi.com/2071-1050/12/12/4845.

22. Lattke, F., K. Larsen, S. Ott and Y. Cronhjort. *Tes energy facade – prefabricated timber based building system for improving the energy efficiency of the building envelope, funded by: Woodwisdom net, research project from 2008-2009*. 2011,
23. Pihelo, P., T. Kalamees and K. Kuusk. "Nzeb renovation with prefabricated modular panels." *Energy Procedia* 132 (2017): 1006-11. https://doi.org/10.1016/j.egypro.2017.09.708. https://www.sciencedirect.com/science/article/pii/S1876610217348592.
24. NKUA, ABT and UNIBO. *D2.6: Sheets on technical data on the case studies*. Task 2.6 - WP2. Pro-GET-onE, 2018,
25. Consulting, M. *Technical assessment report - civil engineering works regarding the change of destination from dormitory to community housing: Str. Zizinului no. 126c, brasov, romania*. Brasov, Romania: 2015,
26. Jeitler, G., M. Augustin and G. Schickhofer. "Birch glt&clt: Mechanical properties of glued laminated timber and cross laminated timber produced with the wood species birch." Presented at WCTE 2016 - World Conference on Timber Engineering, 2016.
27. Wanninger, F. and A. Frangi. "Experimental and analytical analysis of a post-tensioned timber connection under gravity loads." *Engineering Structures* 70 (2014): 117–29. 10.1016/j.engstruct.2014.03.042.
28. Wanninger, F. and A. Frangi. "Experimental and analytical analysis of a post-tensioned timber frame under horizontal loads." *Engineering Structures* 113 (2016): 16-25. 10.1016/j.engstruct.2016.01.029.
29. Priestley, M., S. Sritharan, J. Conley and S. Pampanin. "Preliminary results and conclusions from the presss five-story precast concrete test building." *PCI Journal* 44 (1999): 10.15554/pcij.11011999.42.67.
30. Palermo, A., S. Pampanin, A. H. Buchanan and M. P. Newcombe. "Seismic design of multi-storey buildings using laminated veneer lumber (lvl)." (2005):
31. Granello, G., A. Palermo, S. Pampanin, S. Pei and J. v. d. Lindt. "Pres-lam buildings: State-of-the-art." *Journal of Structural Engineering* 146 (2020): 04020085. doi:10.1061/(ASCE)ST.1943-541X.0002603. https://ascelibrary.org/doi/abs/10.1061/%28ASCE%29ST.1943-541X.0002603.
32. Wanninger, F. *Post-tensioned timber frame structures*. 2015,
33. Wanninger, F. "Fast assembled post-tensioned timber frames." 7e Forum International Bois Construction, FBC 2017, 2017.
34. Systems, B. "Post-tensioning systems." 2021. www.bbv-systems.com. 22 March 2021.
35. Aondio, P., P. Glaser, H. Kreuzinger and P. G. P. Aondio, H. Kreuzinger. "Fe-berechnung von geklebtem brettsperrholz - teil 1: Theorie." *Bauingenieur* 95 (2020): 4.
36. Dujic, B., K. Pirmanšek, R. Zarnić and A. Ceccotti. "Prediction of dynamic response of a 7-storey massive xlam wooden building tested on a shaking table." *World Conference on Timber Engineering* (2010):
37. Gavric, I., M. Fragiacomo and A. Ceccotti. "Cyclic behaviour of typical metal connectors for cross-laminated (clt) structures." *Materials and Structures* 48 (2015): 1841-57. 10.1617/s11527-014-0278-7. https://doi.org/10.1617/s11527-014-0278-7.
38. Sustersic, I., M. Fragiacomo and B. Dujic. "Seismic analysis of cross-laminated multistory timber buildings using code-prescribed methods: Influence of panel size, connection ductility, and schematization." *Journal of Structural Engineering* 142 (2016): E4015012. doi:10.1061/(ASCE)ST.1943-541X.0001344. https://ascelibrary.org/doi/abs/10.1061/%28ASCE%29ST.1943-541X.0001344.
39. CSI. *Etabs ultimate v17.0.1*. Berkeley (CA, USA): Computers & Structures Inc, 2018,
40. (CEN), E. C. o. S. *En 1992-1-1: Eurocode 2: Design of concrete structures - part 1-1: General rules and rules for buildings*. Brussels, Belgium: 2004,
41. (CEN), E. C. o. S. *En 1991-1-1: Eurocode 1: Actions on structures - part 1-1: General actions - densities, self-weight, imposed loads for buildings*. Brussels, Belgium: 2002,
42. (CEN), E. C. o. S. *En 1998-3: Eurocode 8: Design of structures for earthquake resistance - part 3: Assessment and retrofitting of buildings*. Brussels, Belgium: 2005,
43. (CEN), E. C. o. S. *En 1998-1: Eurocode 8: Design of structures for earthquake resistance - part 1: General rules, seismic actions and rules for buildings*. Brussels, Belgium: 2004,
44. Aondio, P., P. Glaser and H. Kreuzinger. "Fe-berechnung von geklebtem brettsperrholz - teil 2: Beispiele." *Bauingenierur* 95 (2020): 4.
45. Giardini, D., J. Woessner and L. Danciu. "Mapping europe's seismic hazard." *Eos, Transactions American Geophysical Union* 95 (2014): 10.1002/2014EO290001.
46. (CEN), E. C. o. S. *En 1995-1-1: Eurocode 5: Design of timber structures - part 1-1: General - common rules and rules for buildings*. Brussels, Belgium: 2004,
47. Kontadakis, A., A. Tsangrassoulis, L. Doulos and S. Zerefos. "A review of light shelf designs for daylit environments." *Sustainability* 10 (2018): 71. https://www.mdpi.com/2071-1050/10/1/71.
48. Van de Kuilen, J. W. G. and Z. Xia. "Lateral behavior of post-tensioned cross laminated timber walls using finite element analysis." WCTE 2014: Proceedings of the World Conference on Timber Engineering, Quebec, Canada, 10-14 August 2014, 2014-08-10. 2014.

urn:NBN:nl:ui:24-uuid:bedab420-3c45-44f6-821e-4ba87ca35f50.

49. Sarti, F., A. Palermo and S. Pampanin. "Quasi-static cyclic testing of two-thirds scale unbonded posttensioned rocking dissipative timber walls." *Journal of Structural Engineering* 142 (2016): E4015005. doi:10.1061/(ASCE)ST.1943-541X.0001291. https://ascelibrary.org/doi/abs/10.1061/%28ASCE%29ST.1943-541X.0001291.